SPEED PERFORMANCE AND CONTROL OF A MICROMACHINED LINEAR BROWNIAN MOTOR

Ersin Altintas[1], Edin Sarajlic[1], Karl F. Böhringer[2], and Hiroyuki Fujita[1]
[1]CIRMM, Institute of Industrial Science, The University of Tokyo, JAPAN
[2]Department of Electrical Engineering, The University of Washington, Seattle, WA, USA
contact: ersin@iis.u-tokyo.ac.jp

ABSTRACT

We report on fabrication and experimental characterization of a linear Brownian motor with a periodic 3-phase electrostatic rectification for unidirectional transport of nanobeads in microfluidic channels. The transport of the beads is performed in 1 μm deep, 2 μm wide PDMS microchannels, which constrain three-dimensional random motion of nanobeads into 1D fluctuation, so-called tamed Brownian motion. 2 μm wide and 4 μm separated ITO electrodes are fabricated by lift-off process on a 24x36 mm^2 coverglass. After planarization of the surface, a previously fabricated PDMS sheet with microchannels is aligned and sealed with the electrodes. Diluted fluorescent nanobead suspension, 1:1000 and 500 nm in diameter, is introduced and equilibrium of the flow is awaited. Experimental results reveal the influence of electrode spacing, switching sequence (excitation time and Brownian time or diffusion time) and viscosity on the transportation and speed performance of the motor. Average speed is dependent on the switching sequence and it peaks around the expected diffusion time of the particles between electrodes.

1. INTRODUCTION

A Linear Brownian Motor (LBM) harvests random thermal fluctuations (Brownian motion), which is one of the dominating phenomena at the nanoscale [1, 2], to fuel transportation of nanoscopic particles thanks to 3-phase electrostatic rectification. Recently, we have devised the first prototype of a micromachined LBM with a 3-phase electrostatic rectification and successfully demonstrated its working principle [3].

Our device employs microchannels to tame, i.e., to limit the 3D random motion of nanobeads into 1D motion, and 3-phase electrodes to rectify the motion (Fig. 1). Here, we improved the design such that we increased the number of electrodes for more convenient transport of the particles over long ranges. The electrodes are 2 μm in width and equally spaced such that they have a 4 μm separation from each other. Electrostatic force should satisfy the following conditions: (i) it is high enough to keep the particle on the electrode against the Brownian motion but (ii) weak and localized enough not to attract the particle directly from an adjacent inactive electrode. Therefore, a bead travels from one electrode to the next by Brownian motion only. With the rectification in one direction, the probability that the bead moves in that direction becomes higher than the opposite one.

2. PRINCIPLE

The working principle of the Brownian motor is given in Fig. 2. A bead is initially trapped on an electrode (a-b). By switching off the voltage, the bead starts Brownian motion and the probability density function becomes wider. The time to make Brownian motion is called
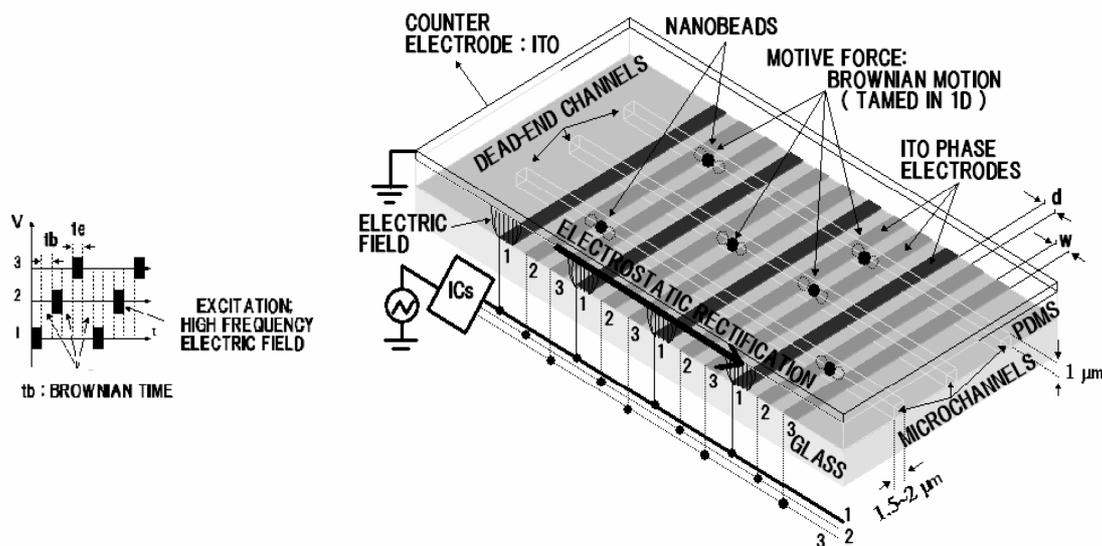
Figure 1. Schematic of improved micromachined linear Brownian motor (LBM). 3D Brownian motion is tamed in microchannels and turned into 1D motion. 3-phase electrostatic field rectifies this random motion. E-field is shown on the left side only. PDMS and glass are not to scale. Two designs were built. LBM-2 with w (electrode width) = d (electrode spacing) = 2μm and LBM-4 with 2w = d = 4μm. t_b : Brownian time of particles to diffuse [OFF-State], t_e : excitation time of each phase [ON-State]).
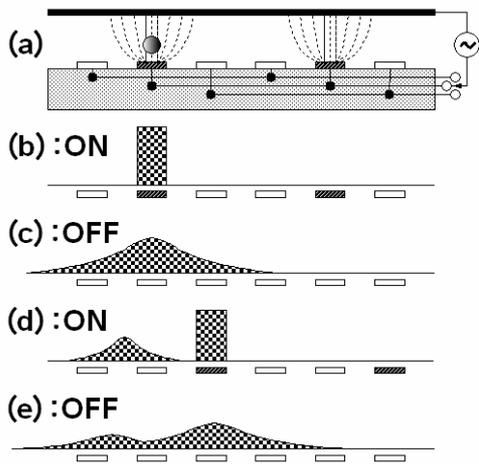
Figure 2. Principle of Brownian motor. 3-phase electrostatic rectification of Brownian motion provides net motion. (a-b) Trapping of the bead. (c) Probability distribution after Brownian motion. (d) Next phase and trapping. (e) Next probability distribution after further Brownian motion.

Brownian time, t_b (c). Then, the electrodes of the next phase are energized with a high frequency electric field. When the bead happens to come to the active electrode, it is trapped on that electrode. The time to trap the particle is called excitation time, t_e (d). By continuing this procedure, the probability of the transportation to the right will be higher than to the left. Since the applied voltage is lower than the one needed for a pure electrostatic transportation, the energy from Brownian motion is utilized in an efficient manner.

3. PHENOMENA AT NANOSCALE

In the system designed, there can be different phenomena causing the motion of the beads apart from Brownian motion and electrostatic force in a high frequency field, which causes dielectrophoretic force on the particle. Those phenomena are mainly gravitational force with buoyancy, AC electroosmosis, thermal flows and electromagnetic forces. Our system operates at high frequency, 1 MHz, and uses 1000 times diluted, 500 nm fluorescent nanobead suspension in DIW, which can be assumed as DIW. Under these specifications, we have estimated the force magnitudes carefully and concluded that the effects of these phenomena are negligible compared to Brownian motion and dielectrophoresis. Therefore, Brownian motion can be exploited for the transportation of nanobeads with the help of electrostatic rectification.

4. FABRICATION

Our experimental device consists of a cover glass with lifted-off ITO electrodes aligned by a PDMS sheet. Electrodes in the design are 2 μm in width and separated by 4 μm. For the electrode fabrication, we selected the photoresist, S1818, due to its relatively high thickness, ~2 μm at 30 sec-3000 rpm, for enhancing the lift-off process. S1818 was patterned and postbaked to withstand the

following BHF processing step. The glass was etched isotropically by BHF almost 100 nm and 100 nm ITO was sputtered. The sample was lifted-off in acetone, and rinsed successively by ethanol and DI water. To increase the conductance, the chip was annealed around 300 °C for 4-6 hours. For a planar surface, hydrophilic OCD solution was spin-coated on the sample and baked by shadowing the pads. PDMS microchannels were prepared from a Si mold whose surface was preprocessed by CHF3 in a RIE system (Samco, RIE-10NR) to enhance the peeling off of PDMS. Mixture was prepared from silicone elastomer:curing agent:FZ77 (500:50:1, Dow Corning). PDMS is hydrophobic; hence we included FZ77 to make it hydrophilic to carry the bead solution spontaneously. After mixing, it was degassed, and poured onto the Si mold, and spin coated. Following this, the sample was cured at 100 °C on a wiper placed on a hot plate. The thickness around the channels was measured as 93±2 μm. PDMS was peeled off, the inlet was opened and the channels with the electrodes were optically aligned (Fig. 3, Union Aligner). The channels are 1 μm deep (bead diameter: 500 nm) and 2 μm wide. As a final step, wire-bonding was performed.

Simulations of the fabricated device using FEMLAB (Fig. 4) revealed that, at 0.25 V (0.5 Vpp), the dielectrophoretic force (DEP force) is sufficient to trap the particle on and near to the electrodes, but it is not sufficient to attract it directly from an inactive adjacent electrode, which is in agreement with the model. The black horizontal line shows the threshold force; thermal energy divided by diameter of the particle, for the field to overcome the Brownian motion. The DEP force peaks at the corners due to fringing fields. However, its cubic dependence on the distance causes sharp decreases when the particle is away from the electrode.

5. EXPERIMENTS AND DISCUSSIONS

Experiments were observed by an inverted microscope (Olympus IX71). The aligned sample was fixed onto a pinch board that had a hole for the objective of the microscope. The sample was fixed onto the stage of the
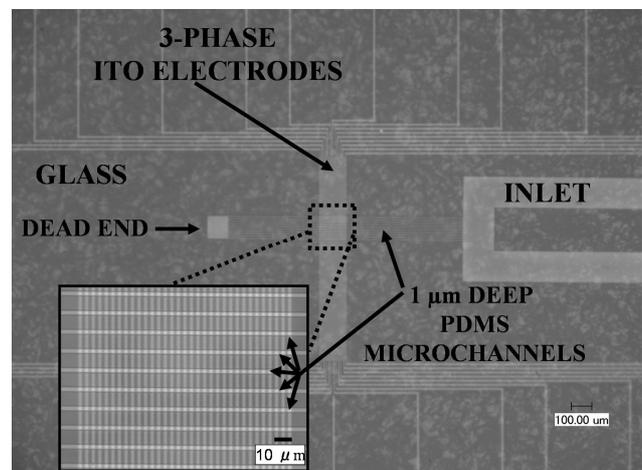

Figure 3. Keyence digital microscope image (VHX-500). PDMS dead-end channels are aligned with 11 sets of 3-phase ITO electrodes (LBM-2, 2 μm electrode spacing). Rectification is to the inlet side.
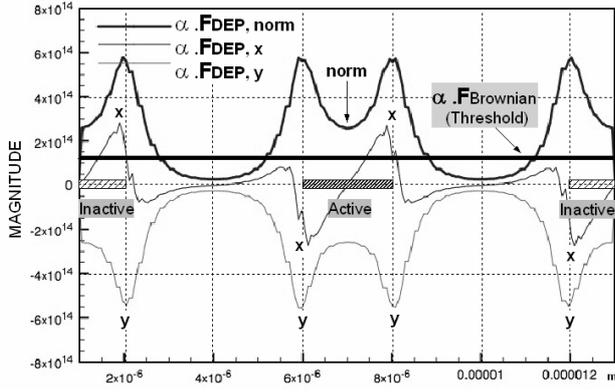
Figure 4. FEMLAB simulation result around active electrode at 0.25 V. DEP force overcomes the Brownian motion of the particle over and near to the electrode. However, it is not enough to attract the particle from an adjacent inactive electrode. Simulation agrees with the model.

Figure 5. Decrease in electrode spacing improves the transportation of nanobeads in microfluidic channels. But, decrease in excitation time t_e degrades it. Curves are polynomial fittings. (All are with DIW. 1-cycle = $3×(t_e + t_b)$.)

microscope and electrical connections were provided. Experiments were recorded (Sony DVD recorder, RDR-HX10) and then analyzed for net-displacements (distance between final position and initial position).

Diluted fluorescent nanobead solution (Fluoresbrite plain microspheres, 2.5% solid latex, 0.5 μm, YG, Polysciences Inc., 1:000-Original:DIW) with water was injected into the inlet and then it was left until stabilization was achieved. The counter ITO electrode consisting of coverglass whose both sides are sputter-coated by ITO with a good conductance was placed on the PDMS sheet. 1D random motion of the beads was confirmed by the optical microscope.

We have investigated the performance of the improved systems in terms of *electrode spacing, viscosity, η, Brownian time, t_b, and excitation time, t_e*, by taking the chip with 4 μm electrode spacing as a reference chip and named it LBM-4. The voltage and the frequency were fixed to 0.5 Vpp and 1 MHz, respectively. In the experiments, net displacements are calculated for a sufficient number of beads (between 80 and 170) and they are rounded to the nearest integer values of 4. Distributions are obtained for 5 full-cycles (5×3×(Brownian time + Excitation time), e.g. 5×3×(4+4)=120 s). This actually implies the investigation of speed performance of the system for per 5 full-cycles. In all experiments, this cycle was kept constant, not the experiment time.

Figure 5 shows the effect of electrode spacing and excitation time. When spacing is 2 μm, LBM-2, the average of the net-displacements is two times larger than that of LBM-4, which shows better performance in terms of transportation. It is easier for particles to diffuse from one electrode to another and also the DEP force is larger due to small gap (8 times) compared to LBM-4 μm. Those would affect the displacements where the voltage is kept as fixed. The transportation performance is dependent on t_e which represents the effect of electrostatic rectification. At longer time durations of activation, particles are more likely to reach the active electrodes by diffusion and to be trapped by the field. Therefore, the displacement would be larger. Furthermore,
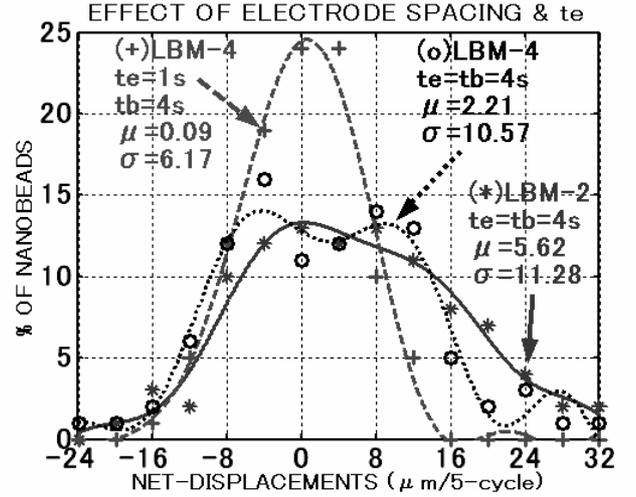
we have worked on 5-cycle, so the total time of the experiments are different (t_e = 1s & 4s). Hence, smaller displacements are expected for small duration of excitation times.

Another parameter for the performance of the motor is viscosity. Brownian motion has an inverse relationship with the viscosity of the medium. In a more viscous medium, drag force prevents longer range displacements and it is difficult for the particles to cross the distance between electrodes (Eq. 1) and therefore the average value of the displacements is smaller (Fig. 6). The ratio of the square of the means of the systems with different media $(2.21/1.44)^2 = 2.35 ∼ 2.2$ is in good agreement with the ratio of the viscosities of the medium (Eq. 1). Less viscous media will increase the displacements, and so improve the performance of the transportation.

$$<X^2>=2Dt_b, \text{ where } D=(k_B T)/(6\pi r\eta) \qquad (1)$$

X: rms Brownian displacement, D: Diffusion constant, k_B: Boltzmann constant, T: Temperature (298 K), r: Radius of the particle (250 nm), η: Viscosity

The last parameter that we have experimentally checked is the effect of Brownian time, t_b, of the system. To investigate t_b, t_e was kept as 4 seconds due to larger and observable displacements. t_b improves the transportation performance of the system (Fig. 7). Comparison of Brownian times t_b = 0, 4 and 8 seconds reveals that displacements are strongly dependent on Brownian motion. During the time t_b, it is in OFF state, and there is no excitation. The particles are free to diffuse in the microchannels in one way. Figure 7 shows that t_b changes performance of the motor significantly. As t_b is increased, the particles are diffused more, and this is clear from the standard deviations of the distributions. For increasing t_b, the system spreads more for a fixed excitation cycle. However, one can consider how much we can improve the performance of the motor by increasing Brownian time of the system. To figure out

performance and its dependence on t_e and t_b, we have investigated the average speed of LBM-4 over the total time of each experiment. The result (Fig. 8) indicates that performance is strongly dependent on both of the parameters and it reaches a peak, which approximately coincides with the expected Brownian time of the particles between the electrodes (electrode spacing in fabricated device is around 3.5 µm, Eq. 1). Increasing t_e would probably increase the average speed. Even though increasing t_b can increase the displacements and so the average value, the average speed of the overall system would decrease. Increasing t_b further would not improve the average speed of the motor.
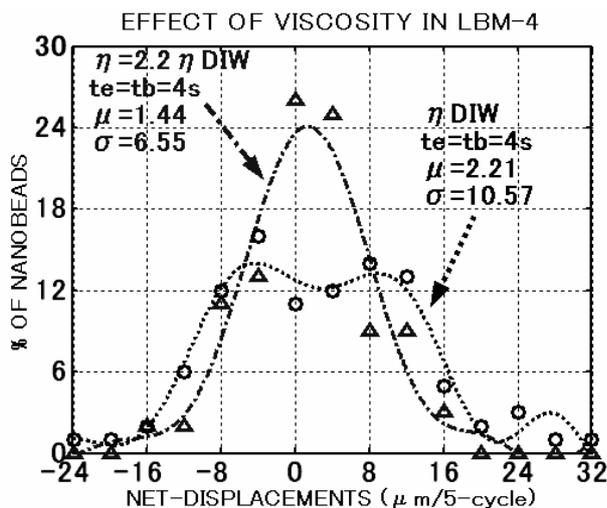
Figure 6. Viscous medium decreases displacements of nanobeads in the microchannels. Hence, the performance degrades. Curves are polynomial fittings (1-cycle=3×(t_{e} + t_{b})).
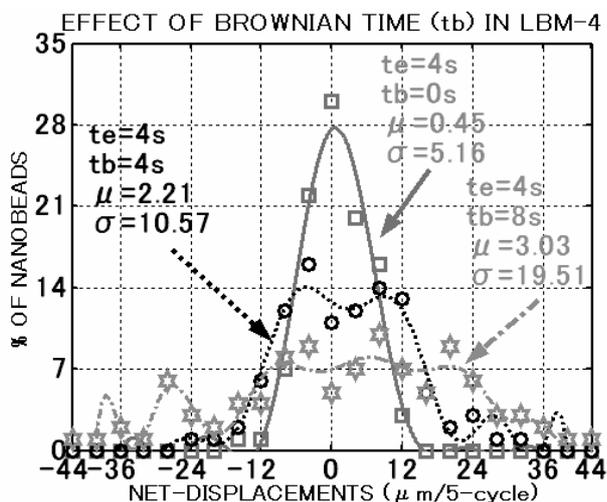
Figure 7. Brownian time, diffusion time of particles in OFF state, improves the performance significantly (LBM-4 d=4 µm). Larger displacements are clear with t_b (Larger σ). Curves are polynomial fittings. (All are with DIW. t_e = 4 s, but t_b = 0, 4 and 8 s respectively. 1-cycle=3×(t_{e} + t_{b}).)
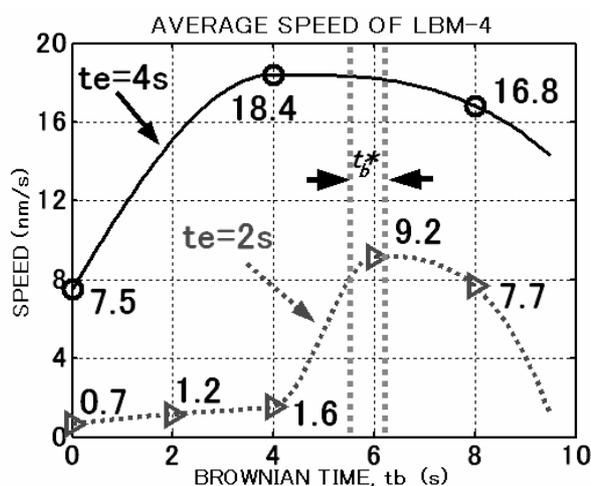
Figure 8. Average speed of LBM-4 (d=4 µm) over total time. It peaks near the expected diffusion time t_b* for a particle between electrodes (region between dotted vertical lines). Performance decreases with excitation time. Speed is controllable. (Curves are fittings.)

6. CONCLUSION

We have experimentally investigated and characterized the influence of electrode spacing, viscosity, and switching sequence on the speed and transportation performance of a micromachined linear Brownian motor. Those are crucial to manipulate nanoparticles effectively and efficiently to exploit and rectify their random thermal motion. Currently we are working on mapping and implementing a rotary Brownian motor. It is thought that this might lead to artificial nanomotors that could be compared with natural biomotors.

7. ACKNOWLEDGEMENTS

8. REFERENCES

[1] R. D. Astumian, "Making Molecules into Motors", Sci. Am., V. 285, pp. 56-64, 2001.
[2] P. Hanggi, F. Marchhesoni and F. Nori, "Brownian Motors", Ann. Phys., V.14, No.1-3, pp.51-70, 2005.
[3] E. Altintas, K. F. Böhringer and H. Fujita, "Micromachined Linear Brownian Motor: Net-unidirectional Transport of Nanobeads by Tamed Brownian Motion with Electrostatic Rectification", IEEE-MEMS Conference, pp. 839-842, Kobe, Japan, 2007.